RESEARCH ARTICLE

Key Points:
- We have investigated terpene emissions in the past millennium
- Land cover and CO_2 govern isoprene emission in industrial time
- Monoterpene and sesquiterpene emissions have been driven by temperature

Supporting Information:
- Readme
- Figure S1

Correspondence to:
J. C. Acosta Navarro,
Juan-Camilo.acosta@itm.su.se

Global emissions of terpenoid VOCs from terrestrial vegetation in the last millennium

J. C. Acosta Navarro[1], S. Smolander[2], H. Struthers[3], E. Zorita[4], A. M. L. Ekman[5], J. O. Kaplan[6], A. Guenther[7], A. Arneth[8], and I. Riipinen[1]

[1]Department of Applied Environmental Science and Bolin Centre for Climate Research, Stockholm University, Stockholm, Sweden, [2]Department of Physics, University of Helsinki, Helsinki, Finland, [3]NSC, Linkoping University, Linkoping , Sweden, [4]Institute for Coastal Research, Geesthacht, Germany, [5]Department of Meteorology and Bolin Centre for Climate Research, Stockholm University, Stockholm, Sweden, [6]Institute of Environmental Engineering, Ecole Polytechnique Federale de Lausanne, Lausanne, Switzerland, [7]Atmospheric Sciences and Global Change Division, PNNL, Richland, Washington, USA, [8]Institute of Meteorology and Climate Research, Karlsruhe Institute of Technology, Garmisch-Partenkirchen, Germany

Abstract We investigated the millennial variability (1000 A.D.–2000 A.D.) of global biogenic volatile organic compound (BVOC) emissions by using two independent numerical models: The Model of Emissions of Gases and Aerosols from Nature (MEGAN), for isoprene, monoterpene, and sesquiterpene, and Lund-Potsdam-Jena-General Ecosystem Simulator (LPJ-GUESS), for isoprene and monoterpenes. We found the millennial trends of global isoprene emissions to be mostly affected by land cover and atmospheric carbon dioxide changes, whereas monoterpene and sesquiterpene emission trends were dominated by temperature change. Isoprene emissions declined substantially in regions with large and rapid land cover change. In addition, isoprene emission sensitivity to drought proved to have significant short-term global effects. By the end of the past millennium MEGAN isoprene emissions were 634 TgC yr^{-1} (13% and 19% less than during 1750–1850 and 1000–1200, respectively), and LPJ-GUESS emissions were 323 TgC yr^{-1} (15% and 20% less than during 1750–1850 and 1000–1200, respectively). Monoterpene emissions were 89 TgC yr^{-1} (10% and 6% higher than during 1750–1850 and 1000–1200, respectively) in MEGAN, and 24 TgC yr^{-1} (2% higher and 5% less than during 1750–1850 and 1000–1200, respectively) in LPJ-GUESS. MEGAN sesquiterpene emissions were 36 TgC yr^{-1} (10% and 4% higher than during 1750–1850 and 1000–1200, respectively). Although both models capture similar emission trends, the magnitude of the emissions are different. This highlights the importance of building better constraints on VOC emissions from terrestrial vegetation.

1. Introduction

Terrestrial vegetation emits large amounts of nonmethane organic vapors known as biogenic volatile organic compounds (BVOCs) (700–1000 TgC yr^{-1}) [*Laothawornkitkul et al.*, 2009]. Terpenes $C_{n5}H_{n8}$ (e.g., isoprene, monoterpenes, and sesquiterpenes) are of particular importance because they are abundant in the atmosphere and are chemically very reactive. Present-day estimates of terpene emissions range from 40 to 65% of the total BVOC mass released by vegetation (Table 1) [*Kesselmeier and Staudt*, 1999; *Arneth et al.*, 2008a; *Laothawornkitkul et al.*, 2009; *Guenther et al.*, 2012]. Furthermore, it is estimated that vegetation alone contributes to approximately 90% of the global volatile organic compound emissions [*Guenther et al.*, 2006; *Piccot et al.*, 1992]. BVOCs oxidize in successive reactions in the atmosphere into an extensive array of products which gradually become less volatile. Tropospheric O_3, a potent greenhouse gas and an important air pollutant, is either produced or destroyed in reactions involving BVOCs and their oxidation products mediated by the concentration of NO_x [*Atkinson and Arey*, 2003]. In addition, a significant fraction of the released terpenes is oxidized by OH, affecting the tropospheric concentration of OH and methane (CH_4) [*Fehsenfeld et al.*, 1992].

The emission of BVOCs from terrestrial vegetation is also a key process controlling new particle formation and growth over continental regions [*Carslaw et al.*, 2010; *Riipinen et al.*, 2011; *Kerminen et al.*, 2012; *Makkonen et al.*, 2012] and may in addition play an important role in new particle formation in the upper troposphere [*Ekman et al.*, 2008]. Depending on location, 20% to 90% of the total submicrometer mass of aerosols is organic [*Jimenez et al.*, 2009] and a large fraction of this mass is secondary, i.e., formed in the

Table 1. Atmospheric Concentrations, Lifetimes, and Global Emissions of Biogenic Volatile Organic Compounds (BVOCs)[a]

Compound Family	Chemical Lifetime[b]	Global Emissions (TgC yr^{-1})	Atmospheric Concentrations
Isoprene	Hours	309–706	ppt to several ppb
Monoterpenes	Minutes to hours	26–156	ppt to several ppb
Sesquiterpenes	Minutes	26	parts per quadrillion to ppt
Other reactive VOC	< 1 day	260	1–3 ppb
Other VOC	> 1 day	260	2–30 ppb

[a]Adapted from *Kesselmeier and Staudt* [1999], *Arneth et al.* [2008a], *Laothawornkitkul et al.* [2009], and *Guenther et al.* [2012].

[b]Lifetimes were estimated with $[O_3]$ = 20 ppb and $[OH]$ = 10^6 molecules/cm^3 for daylight conditions; $[NO_3]$ = 10 parts per trillion (ppt) and $[O_3]$ = 20 ppb for night conditions.

atmosphere by conversion from gas to particle phase. Current estimates of the total global Secondary Organic Aerosol (SOA) range between 50 and 380 Tg SOA yr^{-1} [*Spracklen et al.*, 2011]. Additionally, BVOCs and their oxidation products are responsible for the formation of at least 60% of the SOA [*Engelhart et al.*, 2008; *Hallquist et al.*, 2009]. If the atmospheric conditions are appropriate, BVOCs will contribute to a significant fraction of newly formed particles that can grow to form cloud condensation nuclei (CCN) (> 30 nm) [*Riipinen et al.*, 2012]. For a constant liquid water content, a change in the CCN number may affect the albedo, thickness, and lifetime of clouds [*Albrecht*, 1989; *Twomey*, 1977; *Hoyle et al.*, 2009]. Recently, it has also been shown that semivolatile oxidation products of volatile organic compounds within clouds may also significantly enhance droplet number concentrations [*Topping et al.*, 2013]. Historical estimates of BVOC emissions are necessary to understand the pristine loadings of SOA mass [*Andreae et al.*, 2004]. In addition to the climate effects, small aerosol particles (< 100 nm) are suspected to cause serious health consequences over populations continuously exposed to high concentrations [*Madl and Hussain*, 2011].

Under the same atmospheric conditions, different plant species emit a particular BVOC at different emission rates. The inherent BVOC emission rate of a plant species and the species composition over a region is one of the main determinants of the magnitude of the carbon mass released in the form of volatile organic compounds, modulated by short-term responses of different BVOC to light and temperature.

Anthropogenic land cover change has been a major historical transformer of natural ecosystems into crops and pastures. Present-day estimates of modified land by humans range between 30% and 50% of the total land cover of the Earth [*Vitousek et al.*, 1997]. This has caused changes in the BVOC emissions over time, since crops and grasses tend to emit less terpenes compared to forests and woodlands. Table 1 summarizes the present-day estimates of global BVOC emissions, concentrations, and chemical lifetime in the atmosphere based on *Kesselmeier and Staudt* [1999], *Arneth et al.* [2008a], *Laothawornkitkul et al.* [2009], and *Guenther et al.* [2012].

Existing studies that link past emissions of BVOCs to atmospheric properties have looked at few specific periods in the Holocene and emphasize the role of BVOC emissions as key factors regulating the lifetime and abundance of methane after the last glacial maximum [*Kaplan et al.*, 2006; *Valdes et al.*, 2005]. Other studies estimate the isoprene change from preindustrial to present-day and future scenarios, focusing on the SOA yield and impacts on the atmospheric chemistry [*Pacifico et al.*, 2012]. In addition, *Tanaka et al.* [2012] studied the variability of isoprene and monoterpene emissions since the middle of the nineteenth century caused by land cover, temperature, and solar radiation changes. *Wu et al.* [2012] studied the effect of land use, land cover, and climate and CO_2 changes on terpene emissions over the 21st century and found that isoprene and monoterpene emission are expected to increase in the 21st century driven by temperature change. An experimental study on the organic aerosol variability in Europe in the twentieth century was estimated from dissolved organic carbon in Alpine ice cores. The results show a rise in particulate organic matter presumably from biogenic sources such as BVOCs [*Legrand et al.*, 2013].

To our knowledge, no study has focused on the change of BVOC emissions before preindustrial times using high temporal resolution simulations. Our simulations allowed us to compare long- and short-term BVOC emission variability as a result of the climate natural variability and compare it to long-term changes

induced by humans. We also investigated the long-term effect on isoprene emissions of atmospheric carbon dioxide concentration and the response to drought.

This study seeks to answer the following questions: (1) How did changes in land cover, surface air temperature, and carbon dioxide concentrations affect the terpene emissions in the past millennium? (2) What caused the change in emissions of each compound group? (3) How well do estimates agree between the Model of Emissions of Gases and Aerosols from Nature (MEGAN) [*Guenther et al.*, 2012; *Sakulyanontvittaya et al.*, 2008] and The Lund-Potsdam-Jena-General Ecosystem Simulator (LPJ-GUESS) [*Smith et al.*, 2001; *Sitch et al.*, 2003]? Finally, we briefly discuss the potential implications of the changing emissions on atmospheric chemical and physical processes.

2. Methods

2.1. Modeling Terpene Emissions

We calculated and compared emissions over the past millennium using the models MEGAN 2.02 [*Sakulyanontvittaya et al.*, 2008] modified with CO_2 and soil moisture algorithms [*Guenther et al.*, 2012], and LPJ-GUESS [*Smith et al.*, 2001; *Sitch et al.*, 2003]. We carried out sensitivity simulations to single out driving variables and study their impact on the emissions of the different chemical species and compared the MEGAN terpene emission trends in Europe in the past century to Alpine records of deposited organic aerosol.

2.1.1. The MEGAN Simulations

We estimated global emissions of isoprene, monoterpenes, and sesquiterpenes with MEGAN. The simulations included a CO_2 inhibition effect on isoprene [*Heald et al.*, 2009] with the same global CO_2 value for all the grid boxes at a particular time. We ran MEGAN at a temporal resolution of 3 h and spatial resolution of 3.75° × 3.75° (Gaussian 96 × 48 grid) and forced the model with daily mean meteorological data from a simulation with the global climate model Max-Planck-Institut-Earth system model (MPI-ESM) covering the last 1200 years [*Jungclaus et al.*, 2010], yearly mean values of land cover data from the Kaplan-Krumhardt (KK10) vegetation scheme [*Kaplan et al.*, 2010, 2012], and yearly CO_2 concentration values from *MacFarling Meure et al.* [2006].

The Earth system model MPI-ESM consist of the atmosphere model European Cenrte/Hamburg 5, coupled to the ocean model OM and to the global carbon cycle Hamburg Model of the Ocean Carbon Cycle 5 and the land use surface scheme JSBACH. The model was driven by estimations of past external climate forcings: solar variability, volcanic eruptions, greenhouse gases, land cover changes, and stratospheric ozone. The amplitude of variations of past solar irradiance is still debated, and thus, *Jungclaus et al.* [2010] conducted two ensembles of simulations, one driven by a narrow amplitude of variations of the solar constant (about 0.1% of the present value) and one with a wider amplitude (about 0.25% of the present value). More recent estimations of past solar variations seem to cluster around the narrower value, as it was recommended for the millennium simulations participating in the Climate Model Intercomparison Project, version 5 [*Schmidt et al.*, 2011]. Thus, in this study we chose one of the simulations of the narrow-amplitude solar variations. For further technical details about this ensemble of simulations the reader is referred to *Jungclaus et al.* [2010].

The MPI-ESM data includes global daily values of Surface Air Temperature (SAT), Downward Solar Radiation at the Surface (DSRS), Leaf Area Index (LAI), and Soil Water (SW) content with a spatial resolution of 3.75° × 3.75° (Gaussian 96 × 48 grid) [*Jungclaus et al.*, 2010]. The original vegetation maps were upscaled from a spatial resolution of 0.5° × 0.5° [*Kaplan et al.*, 2010, 2012] to the desired 3.75° × 3.75° resolution, and the original 14 Plant Functional Types (PFTs) (11 natural + 3 anthropogenic) were reduced to six general isoprene-emitting PFTs described by *Guenther et al.* [2006] and four general monoterpene and sesquiterpene emitting PFTs with emission factors described by *Sakulyanontvittaya et al.* [2008]. We reduced the 14 PFTs to 6 isoprene-emitting PFTs as follows: C3/C4 pasture = C3 + C4 pasture; crops = crops; shrub = shrub + tundra + natural C3 + C4 grass; temperate/boreal evergreen = temperate evergreen + boreal evergreen; temperate/boreal deciduous = temperate deciduous + boreal deciduous; and broadleaf trees = tropical evergreen + tropical deciduous + temperate evergreen. In the case of monoterpene and sesquiterpene emissions the six PFTs were further reduced by assuming that crops and pastures and temperate/boreal evergreen and temperate/boreal deciduous emit with the same factor, respectively [*Sakulyanontvittaya et al.*, 2008]. Table 2 shows the emission factors of the reduced isoprene, monoterpene, and sesquiterpene PFTs. We assumed annual global CO_2 concentrations inferred from ice cores in Law Dome, Antarctica

Table 2. MEGAN Plant Functional Type (PFT) Classification and Isoprene (IP), Monoterpenes (MT), and Sesquiterpenes (ST) Emission Factors at Standard Conditions[a]

Converted Plant Functional Type	IP Emission Factor	MT Emission Factor	ST Emission Factor
C3/C4 pasture	0.09		
		0.323	0.1
Crops	0.5		
Shrub	10.7	0.735	0.3
Temperate/boreal evergreen	2.0		
		0.872	0.45
Temperate/boreal deciduous	0.7		
Broadleaf trees	12.6	0.449	0.3

[a]MT and ST emission factors are based on *Sakulyanontvittaya et al.* [2008]. IP emission factors are based on *Guenther et al.* [2006]. Factors are in mg (compound) m^{-2} (ground) h^{-1}.

[*MacFarling Meure et al.*, 2006]. A list of the input variables, their origin, and their original spatial and temporal resolution is displayed in Table 3.

Following the general emission equation by *Guenther et al.* [2006], we estimated the above canopy fluxes of isoprene, monoterpenes, and sesquiterpenes in every gridbox as follows:

$$E = \epsilon \times \gamma_{LAI} \times \gamma_T \times \gamma_{age} \times \gamma_{SM} \times \gamma_{CO_2}$$
$$\times ((1 - LDF) + LDF \times \gamma_P) \qquad (1)$$

where E (mg m^{-2} h^{-1}) is the emission rate of a given BVOC. E is determined by the empirical emission factor ϵ (mg m^{-2} h^{-1}) of every PFT (Table 2) at standard conditions as well as by factors γ_{LAI}, γ_T, γ_{age}, γ_{SM}, γ_P, γ_{CO_2}, and a Light Dependency Factor (LDF) for every compound. The factors γ_{LAI}, γ_T, γ_P, γ_{age}, γ_{SM}, and γ_{CO_2} account for changes in the emissions due to deviations from standard conditions and are determined by climate (temperature, solar radiation, and soil water moisture) and land cover (LAI, leaf age) variables. A full description can be found in *Guenther et al.* [2006, 2012].

We parameterized radiation and temperature daily mean values to include daily variations of the variables. We scaled the radiation fields with the solar zenith angle using a scaling coefficient that depends on the latitude and the day of the year, ensuring that the daily average radiation from the parameterization equals the daily average from the MPI-ESM model output. We estimated daily SAT variations using the daily minimum and maximum temperatures from the MPI-ESM model and the parameterization of a daily SAT, where daytime SAT follows a sinusoidal function and nighttime SAT follows a negative exponential function derived by *Parton and Logan* [1981]. The importance of taking into account the daily variability of SAT is discussed in section 3.

Table 3. MEGAN Input Variable List With Respective Origin, Temporal, and Spatial Resolution[a]

Variable Name	Units	Data Origin	Temporal Resolution	Spatial Resolution
SAT	°K	MPI-ESM	Daily mean values	3.75° × 3.75°
DSRS	W m^{-2}	MPI-ESM	Daily mean values	3.75° × 3.75°
LAI	m^2 m^{-2}	MPI-ESM	Monthly mean values	3.75° × 3.75°
SW	m^3 m^{-3}	MPI-ESM	Monthly mean values	3.75° × 3.75°
CO$_2$	ppmv	Law Dome Antarctica	Yearly mean values	1 global value
PFTs	Cover %	KK10	Yearly mean values	0.5° × 0.5°
WP	m^3 m^{-3}	MEGAN	Present-day values	0.5° × 0.5°

[a]Variables: Surface Air Temperature (SAT), Downward Solar Radiation at the Surface (DSRS), Leaf Area Index (LAI), Soil Water (SW) content (3 m of bottom and 3 m of top soil layer values averaged) [*Jungclaus et al.*, 2010], Carbon dioxide concentration (CO$_2$) [*MacFarling Meure et al.*, 2006], 14 Plant Functional Types (PFT) (11 natural + 3 anthropogenic) [*Kaplan et al.*, 2010, 2012], and Wilting Point (WP) [*Guenther et al.*, 2006].

Table 4. LPJ-GUESS Plant Functional Type (PFT) Classification and Isoprene (IP), Monoterpenes (MT) Emission Factors at Leaf Level [*Arneth et al.*, 2008a] Factors are in $\mu g(C)\ g^{-1}$ (Leaf Foliar Mass) h^{-1}

Plant Functional Type (PFT)	IP Emission Factor	MT Emission Factor
Boreal needle-leaved evergreen tree, shade-tolerant	8	4.8
Boreal needle-leaved evergreen tree, shade-intolerant	8	4.8
Boreal needle-leaved summer green tree, shade-intolerant	8	4.8
Shade-tolerant temperate broad-leaved summer green	45	1.6
Shade-intolerant broad-leaved summer green	45	1.6
Temperate broad-leaved evergreen tree, shade-tolerant	24	1.6
Tropical broad-leaved evergreen tree, shade-tolerant	24	0.8
Tropical broad-leaved evergreen tree, shade-intolerant	24	0.8
Tropical broad-leaved rain green tree, shade-intolerant	45	2.4
C3 herbaceous	16	1.6
C4 herbaceous	8	2.4

2.1.2. The LPJ-GUESS Simulations

LPJ-GUESS computes the establishment, growth, and mortality of potential natural vegetation, as well as plant and soil water status and plant litter accumulation on a global scale. Carbon, water, and surface energy exchanges are computed on a daily time step, while establishment, growth and allocation, and mortality by general disturbance and competition are simulated with a yearly time step [*Smith et al.*, 2001; *Sitch et al.*, 2003]. The global version of LPJ-GUESS with 11 PFTs was used, comprising nine tree and two grass PFTs. LPJ-GUESS runs in cohort mode, where groups of individuals of similar age and size, or cohorts are represented by a single individual. We ran LPJ-GUESS with 25 patches per grid cell, and a stochastic general patch-destroying disturbance with an average return interval of 100 years [*Smith et al.*, 2001].

Past climate simulations from the MPI/University of Wisconsin-Madison Earth system model served to drive LPJ-GUESS [*Mikolajewicz et al.*, 2007]. We applied Climate from the Climatic Research Unit of the University of East Anglia for the twentieth century [*Mitchell and Jones*, 2005]. CO_2 concentrations were taken from ice core data, extended by atmospheric observations [*Keeling*, 1960; *Keeling and Piper*, 1996; *Etheridge et al.*, 1996]. We applied a 1000 year model spin-up, using 10 patches to account for stochastic processes related to plant growth and mortality. The LPJ-GUESS emissions submodel for BVOCs is able to compute emission for isoprene and monoterpenes. The formulations have been adopted from the emission algorithms of *Niinemets et al.* [1999] and *Arneth et al.* [2007a, 2008a]. Each PFT is associated with a fraction of electrons absorbed by its leaves. The production is specified for standard environmental conditions and related to the emission capacities used. Table 4 displays the emission capacity at standard environmental conditions in LPJ-GUESS simulations. The reason for the different units in the emission factors given in Table 2 (for MEGAN) and Table 4 (for LPJ-GUESS) is the fundamental difference between the two models: while MEGAN uses canopy scale emission factors, LPJ-GUESS uses leaf level emission factors.

LPJ-GUESS takes into consideration the direct and indirect process response of BVOC emissions to changing climate and CO_2 concentration, including responses at both the leaf and ecosystem scale [*Arneth et al.*, 2007a, 2008b]. In case of monoterpenes, herbaceous and needle-leaved PFTs were assumed to store a fraction of monoterpenes produced and release emissions from storage [*Schurgers et al.*, 2006, 2009b, 2009a].

2.2. Model Setup

We conducted nine MEGAN simulations and two LPJ-GUESS simulations (Table 5). Simulations 1–5 were carried out to test the individual BVOC emission sensitivity of MEGAN. In simulations 1–5 the vegetation and climate conditions were those of the last decade of the past millennium and the model was forced with a control climate simulation in which natural and anthropogenic climate forcing were kept constant, apart from the daily and annual cycles. Simulation 1 (MC-REF) is a basic simulation. In this simulation MEGAN was driven with constant present-day daily temperature, radiation fields, and land cover; and the effects of soil moisture, daily temperature variation, and CO_2 were not included. In simulations 2 (MC-SAT_ON), 3 (MC-VEG_ON), 4 (MC-SW_ON), and 5 (MC-CO2_ON) the conditions are the same as in 1 (MC-REF), but SAT daily cycle parameterization, land cover change (VEG), Soil Water (SW) content parameterization (only for isoprene) and CO_2 parameterization were turned on, each one at a time. These comparisons allowed us to constrain the sensitivity of the emissions to the different modeling schemes in the present climate.

Table 5. In Simulations 1–5 We Drove MEGAN With a Control MPI-ESM Simulation at Present-Day Conditions in Which All Natural and Anthropogenic Climate Forcings Were Not Considered[a]

Simulation ID	Natural + Anthropogenic Climate Forcing	Daily SAT Parameterization	Changing Vegetation	Soil Moisture	CO_2 Concentration
MC-REF	Off	Off	Off	Off	Off
MC-SAT_ON	Off	ON	Off	Off	Off
MC-VEG_ON	Off	Off	ON	Off	Off
MC-SW_ON	Off	Off	Off	ON	Off
MC-CO2_ON	Off	Off	Off	Off	ON
MF-VEG_OFF	On	On	OFF	On IP/OFF MT and ST	On
MF-ALL_ON	On	On	On	On IP/OFF MT and ST	On
MF-VEG_OFF-CO2_OFF	On	On	OFF	On IP/OFF MT and ST	OFF
MF-CO2_OFF	On	On	On	On IP/OFF MT and ST	OFF
LF-CO2_OFF	On	-	On	-	OFF
LF-CO2_ON	On	-	On	-	On

[a]In simulations 6–9 we forced MEGAN with a millennial simulation of MPI-ESM in which all climate forcings were included. The MEGAN control climate and MEGAN forced climate simulations are abbreviated as MC- and MF-, respectively. The last two simulations were done by forcing the model LPJ-GUESS with climate data before 1900 from MPI/UW model with natural and anthropogenic climate forcing, and from Climate Research Unit (CRU) twentieth century climate fields otherwise.

To include the impacts of changing climate, we forced MEGAN with a transient millennial climate simulation including natural and anthropogenic forcing in simulations 6 (MF-VEG_OFF), 7 (MF-ALL_ON), 8 (MF-VEG_OFF-CO2_OFF), and 9 (MF-CO2_OFF). We compared the emission response of land cover change effect in simulation 7 (MF-ALL_ON) versus fixed land cover in simulation 6 (MF-VEG_OFF), keeping all other effects on, where the former represents the case where vegetation is allowed to change dynamically and the latter the case where it is kept constant at initial conditions. These simulations allowed us to study the relative importance of changing climate and vegetation cover for the emission estimates. Analogously, simulations 8 (MF-VEG_OFF-CO2_OFF) and 9 (MF-CO2_OFF) are the same as simulations 6 (MF-VEG_OFF) and 7 (MF-ALL_ON) with the CO_2 effect off, allowing us to single out the relative importance of the CO_2 for the emission predictions.

The effects of land cover and CO_2 on emissions are anthropogenic in nature, whereas the daily SAT cycle and soil water effect are improvements of the model. In simulations 1–5 we investigate the sensitivity of the emissions to both the anthropogenic effects as well as the sensitivity of emissions to model improvements, allowing us to quantify the importance of using the improved version of the model. In simulations 6–9 we used the improved version of MEGAN, forced the model with a changing climate, and tested only the effects of land cover and CO_2 changes.

LPJ-GUESS simulations were performed including changes in land cover adopting the approach by *Olofsson and Hickler* [2008], with time periods between changes in land cover getting progressively shorter toward the present, from 100 year to 10 year resolution. Simulations 10 (LF-CO2_OFF) excluded a CO_2 effect on emissions, whereas simulations 11 (LF-CO2_ON) included the effect.

Observations indicate that higher CO_2 concentrations inhibit production of isoprene in most isoprene-emitting species [*Heald et al.*, 2009; *Monson et al.*, 2007], even though underlying leaf metabolic mechanisms are not yet fully understood [*Peñuelas and Staudt*, 2010]. Although a similar CO_2 inhibition effect has not been observed on monoterpene and sesquiterpene emitting species [*Peñuelas and Staudt*, 2010], the similarity between isoprene and monoterpene metabolic pathways indicate that the CO_2 inhibiting effect could also affect at least monoterpene emissions [*Arneth et al.*, 2011; *Niinemets et al.*, 2010]. Therefore, the results of monoterpene and sesquiterpene emission sensitivity to CO_2 are shown in section 3.1, but the "best estimates" of monoterpene emissions in MEGAN and LPJ-GUESS and sesquiterpene emissions in MEGAN do not include a CO_2 effect.

Field measurements indicate that below a certain soil moisture threshold, the stomatal conductance and photosynthesis of plants decreases. Isoprene emissions are affected by low biologic activity due to inadequate soil moisture levels [*Guenther et al.*, 1999]. Most monoterpenes and sesquiterpenes are emitted from storage pools, and the SW effect modeled on isoprene is not applicable to monoterpene and sesquiterpene emissions. Therefore, the SW effect was applied exclusively to isoprene emissions in the MEGAN simulations,
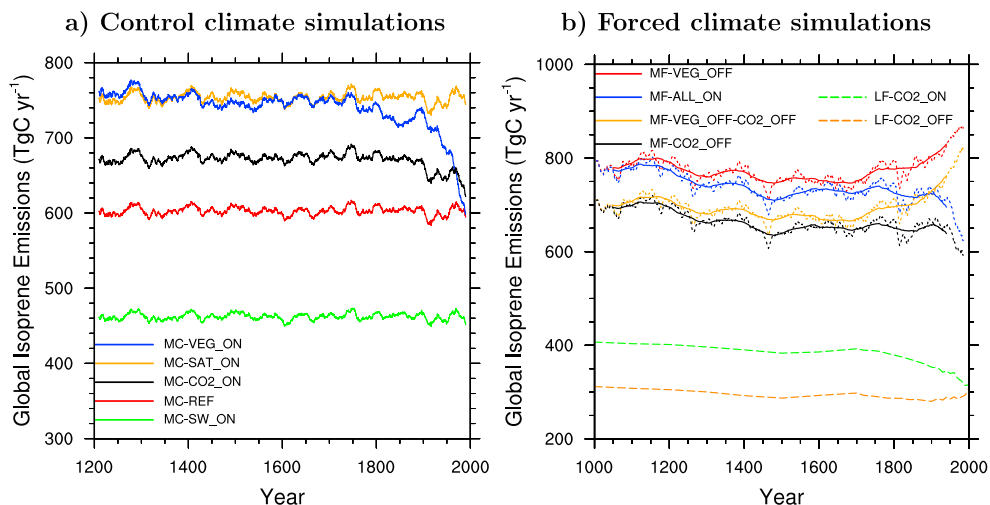
Figure 1. (a) Time evolution of the mean global isoprene emissions in the control climate simulations: 1 (MC-REF) (red), 2 (MC-SAT_ON) (yellow), 3 (MC-VEG_ON) (blue), 4 (MC-SW_ON) (green), and 5 (MC-CO2_ON) (black). The series represent smooth, mean decadal monthly values. (b) Time evolution of the mean global isoprene emissions in the forced simulations. 6 (MF-VEG_OFF) (red), 7 (MF-ALL_ON) (blue), 8 (MF-VEG_OFF-CO2_OFF) (yellow), 9 (MF-CO2_OFF) (black), 10 (LF-CO2_OFF) (orange), and 11 (LF-CO2_ON) (green). MEGAN solid series represent smooth, mean centennial monthly values, and MEGAN dotted series represent smooth, mean decadal monthly values. LPJ-GUESS series have 100 year resolution from 1000 to 1700, 20 year resolution from 1700 to 1900, and 10 year resolution from 1900 to 2000. See Table 5 for a description of the different simulations.

following *Guenther et al.* [2006]. LPJ-GUESS includes the soil water effect on BVOC emissions indirectly in all simulations, by taking into consideration water stress on plant photosynthesis that manifests in the production of BVOCs. However, since monoterpene and sesquiterpene emissions are emitted from storage in herbaceous and needle-leaved plants, water stress has only a partial effect on monoterpene and sesquiterpene emissions in this model.

3. Results and Discussion
3.1. Sensitivity of Global Terpene Emissions to Environmental Stresses
3.1.1. Isoprene Emissions
The temporal evolution of the mean global isoprene emissions estimated with MEGAN in the control climate simulations (MC in Table 5) is displayed in Figure 1a. Simulation 1 (MC-REF) represents the mean global isoprene emissions with fixed land cover and climate from year 1990, and SW, CO_2, and daily cycle of SAT effects were excluded. The short-term variability in emissions is caused by the temperature variability in the climate model. Simulation 2 (MC-SAT_ON) represents isoprene emissions under the same conditions as in simulation 1 (MC-REF) but including a daily SAT cycle. Under this scenario, the emissions are approximately 25% higher than in 1 (MC-REF). Simulation 3 (MC-VEG_ON) represents isoprene emissions when MEGAN is forced with changing land cover. The simulations show that neglecting temperature, radiation, and CO_2 changes, the global isoprene emissions would be about 27% larger at the beginning of the millennium and about 20% larger in 1850 than during present-day conditions. Simulation 4 (MC-SW_ON) is a test of the sensitivity of isoprene emissions to drought. This simulation shows that including a soil water content parameterization may decrease the total isoprene emissions by about 24% as compared to simulation 1 (MC-REF). Simulation 5 (MC-CO2_ON) represents the isoprene emission response of emitting plants to changing atmospheric CO_2. An increase of about 11% is seen from 1200 to 1800 when a CO_2 effect is considered. After 1800, the difference in total isoprene emissions decreases from +11% in 1800 to +4% in 1990 as compared to 1 (MC-REF) simulation.

Figure 1b shows the temporal evolution of the mean global isoprene emissions in the MEGAN and LPJ-GUESS forced climate simulations. The results from the MEGAN simulations are discussed first. Simulation 6 (MF-VEG_OFF) shows how the emissions would have evolved if land cover conditions were kept fixed but climate variables and CO_2 changed. By the end of the twentieth century the total isoprene emissions in the fixed vegetation scenario (6 (MF-VEG_OFF)) would increase as compared to preindustrial times
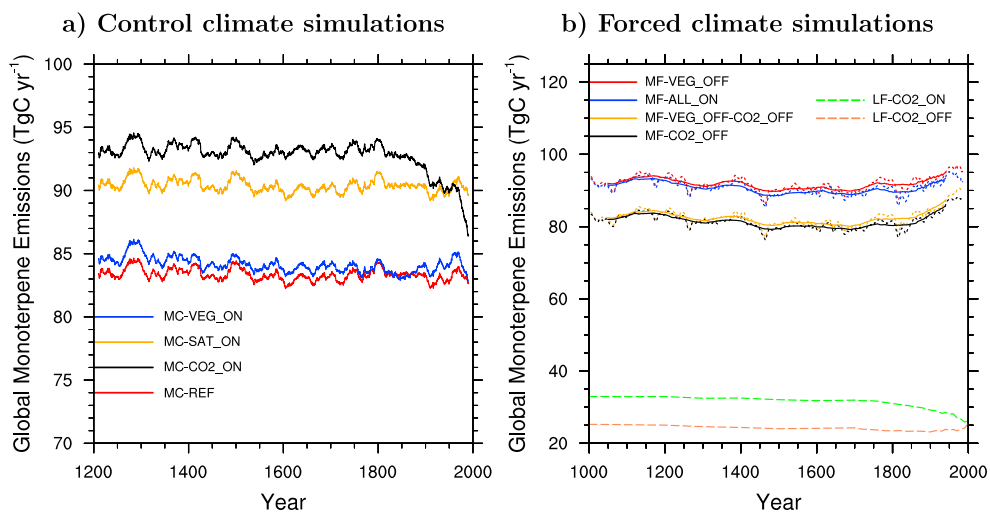
Figure 2. (a) Time evolution of the mean global monoterpene emissions in the control climate simulations: 1 (MC-REF) (red), 2 (MC-SAT_ON) (yellow), 3 (MC-VEG_ON) (blue), and 5 (MC-CO2_ON) (black). The series represent smooth, mean decadal monthly values. (b) Time evolution of the mean global monoterpene emissions in the forced simulations: 6 (MF-VEG_OFF) (red), 7 (MF-ALL_ON) (blue), 8 (MF-VEG_OFF-CO2_OFF) (yellow), 9 (MF-CO2_OFF) (black), 10 (LF-CO2_OFF) (orange), and 11 (LF-CO2_ON) (green). MEGAN solid series represent smooth, mean centennial monthly values, and MEGAN dotted series represent smooth, mean decadal monthly values. LPJ-GUESS series have 100 year resolution from 1000 to 1700, 20 year resolution from 1700 to 1900, and 10 year resolution from 1900 to 2000. See Table 5 for a description of the different simulations.

(1750–1850) by approximately 8%, whereas in the land cover change scenario (7 (MF-ALL_ON)) the total isoprene emissions decreased approximately 13% from the end of preindustrial times to present day. This highlights the importance of the impact of agricultural activity on isoprene emissions in the past millennium in the MEGAN simulations. It can be seen in the series 8 (MF-VEG_OFF-CO2_OFF) that isoprene emissions in MEGAN are dominated by SAT changes, if no land cover change is allowed. Including an atmospheric CO_2 effect on isoprene emissions in MEGAN simulations results in an increment in the emissions, evident by comparing the results from simulations 9 (MF-CO2_OFF) and 7 (MF-ALL_ON), or 8 (MF-VEG_OFF-CO2_OFF) and 6 (MF-VEG_OFF). Independently of including or excluding a CO_2 effect, the effect of changing versus fixed land cover determines the millennial change of the emissions.

The LPJ-GUESS simulations show somewhat different results to the ones from MEGAN (Figure 1b). Simulation 10 (LF-CO2_OFF) with changing climate and land cover, but fixed present-day CO_2, results in 5% higher emissions during present-day than during 1750–1850. When the CO_2 effect is switched on (11 (LF-CO2_ON)), the global present-day emissions decrease 15% as compared to 1750–1850 emissions, illustrating the importance of CO_2 as isoprene emission controller in the LPJ-GUESS model. Additionally, LPJ-GUESS isoprene emissions are about half of MEGAN emissions, likely due to the large differences in the standard emission capacity for each typical PFT and the use of different climate drivers. It is worth noting that the temporal variability within models and the effects of each variable on the emissions are always smaller than the difference between models.

3.1.2. Monoterpene Emissions

Figure 2a displays the temporal evolution of the mean global monoterpene emissions from MEGAN in the control climate simulations (simulations MC in Table 5). The individual external effects on global monoterpene emissions differ from the effects on isoprene in two main aspects. First, comparing simulation 1 (MC-REF) with simulation 3 (MC-VEG_ON), it is evident that the land cover effects observed on isoprene emissions (Figure 1a) were not present in the monoterpene emissions (Figure 2a). MEGAN predicts a small difference between a changing vegetation scenario and the one with fixed vegetation in terms of monoterpene emissions, because the monoterpene standard condition emission factors from crops and pastures as compared with the natural vegetation are of the same order of magnitude (Table 2). Natural vegetation isoprene emission factors, on the contrary, are on average more than 10 times larger than crop and pasture emission factors. Another feature observed is the smaller effect of a daily SAT cycle on global monoterpene emissions as compared with isoprene emissions, 2 (MC-SAT_ON) and 1 (MC-REF) in Figures 2a and 1a,
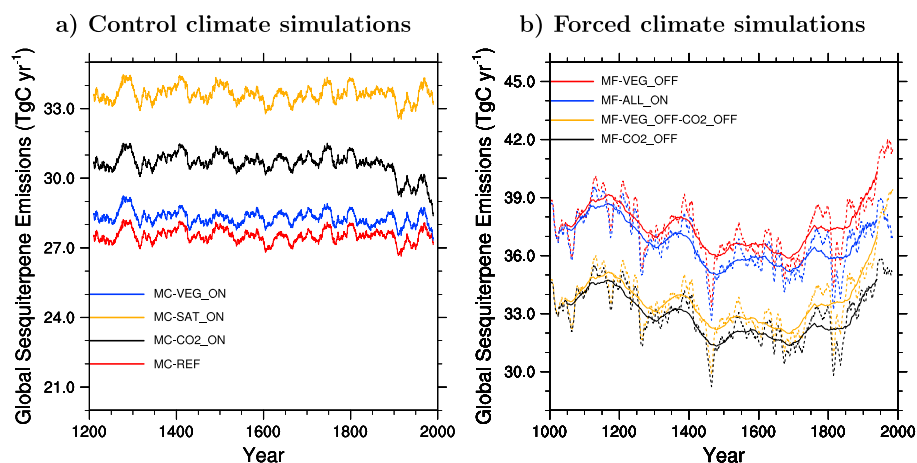
Figure 3. (a) Time evolution of the mean global sesquiterpene emissions in the control climate simulations: 1 (MC-REF) (red), 2 (MC-SAT_ON) (yellow), 3 (MC-VEG_ON) (blue), and 5 (MC-CO2_ON) (black). The series represent smooth, mean decadal monthly values. (b) Time evolution of the mean global sesquiterpene emissions: 6 (MF-VEG_OFF) (red), 7 (MF-ALL_ON) (blue), 8 (MF-VEG_OFF-CO2_OFF) (yellow), and 9 (MF-CO2_OFF) (black). The solid series represent smooth, mean centennial monthly values, and the dotted series represent smooth, mean decadal monthly values. See Table 5 for a description of the different simulations.

respectively. Monoterpene emissions were about 9% higher when a daily SAT cycle is taken into account, because intradaily temperature differences at higher latitudes are smaller on average than at lower latitudes and the fraction of monoterpene emissions from high-latitude vegetation to total global monoterpene emissions is much larger than the respective isoprene fraction. The results from simulation 5 (MC-CO2_ON) in Figure 2a indicate that global monoterpene emissions would have a similar response as global isoprene emissions to CO_2 if the mechanism was found to be true for monoterpenes.

Figure 2b shows the temporal evolution of the mean global monoterpene emissions in the forced simulations for both MEGAN and LPJ-GUESS (last six simulations in Table 5). Simulation 8 (MF-VEG_OFF-CO2_OFF) indicates the temporal evolution of monoterpene emissions with fixed vegetation from year 1000, changing climate and no effect of CO_2. The relative difference in global monoterpene emissions between a fixed vegetation scenario (8 (MF-VEG_OFF-CO2_OFF)) in the end of the twentieth century and the 1750–1850 emission average is about +11%, while the same relative difference in a changing vegetation scenario (9 (MF-CO2_OFF)) is about +10%, a much smaller change than the equivalent isoprene case shown in Figure 1b and discussed above.

LPJ-GUESS monoterpene emissions (11 (LF-CO2_ON) and 10 (LF-CO2_OFF)) show the same behavior as LPJ-GUESS global isoprene emissions, i.e., CO_2 would be the main controller of the millennial variability, and the magnitude is about one third of MEGAN emissions for similar reasons as isoprene emissions.

3.1.3. Sesquiterpene Emissions

The MEGAN sesquiterpene emissions sensitivity to different forcings is in general similar to the sensitivity of the monoterpene emissions. However, when including a SAT cycle, sesquiterpene emissions change considerably. The mean global emissions in 2 (MC-SAT_ON) in Figure 3a are about 21% larger than in the simulation 1 (MC-REF), due to a higher temperature sensitivity of sesquiterpene emissions. The full effect of a changing vegetation in a changing climate scenario on global sesquiterpene emissions is seen by comparing simulation 8 (MF-VEG_OFF-CO2_OFF) and simulation 9 (MF-CO2_OFF) in Figure 3b. A fixed 1000 vegetation represents 17% larger emissions by the end of the twentieth century as compared to the 1750–1850 global mean, whereas emissions were about 10% larger in the end of the twentieth century than between 1750 and 1850 with a changing vegetation scenario. Uncertainty in sesquiterpene emissions is larger than isoprene or monoterpene emissions, because fewer measurements exist.

The sensitivity analysis presented above allowed us to identify environmental factors driving the long-term changes in isoprene, monoterpene, and sesquiterpene emissions in the past millennium. The effects of land cover change (crops and pastures) and carbon dioxide dominate over temperature on global isoprene emissions, while temperature has a larger impact than land cover on monoterpene and sesquiterpene emissions.
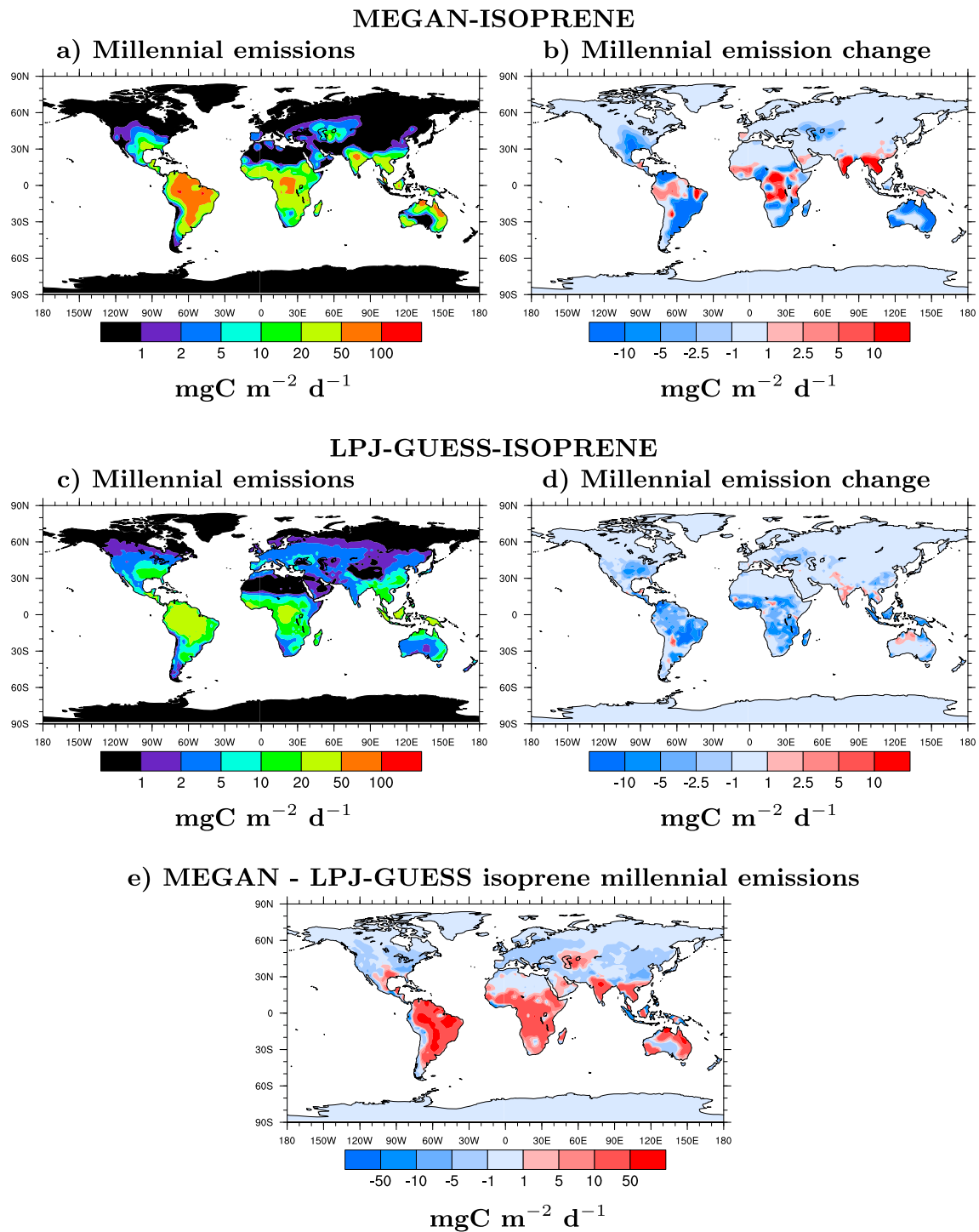
MEGAN-ISOPRENE

a) Millennial emissions b) Millennial emission change

c) Millennial emissions d) Millennial emission change

LPJ-GUESS-ISOPRENE

e) MEGAN - LPJ-GUESS isoprene millennial emissions

Figure 4. (a) Time-averaged millennial isoprene emissions in simulation 7 (MF-ALL_ON). (b) Difference between time-averaged present-day (1980–1990) and time-averaged (1000–1010) isoprene emissions in simulation 7 (MF-ALL_ON). (c) Time-averaged millennial isoprene emissions in simulation 11 (LF-CO2_ON). (d) Difference between time-averaged present-day (1995–2005) and 950–1050 isoprene emissions in simulation 11 (LF-CO2_ON). (e) Millennial absolute difference between MEGAN isoprene emissions in simulation 7 (MF-ALL_ON) and the LPJ-GUESS 11 (LF-CO2_ON) simulation.
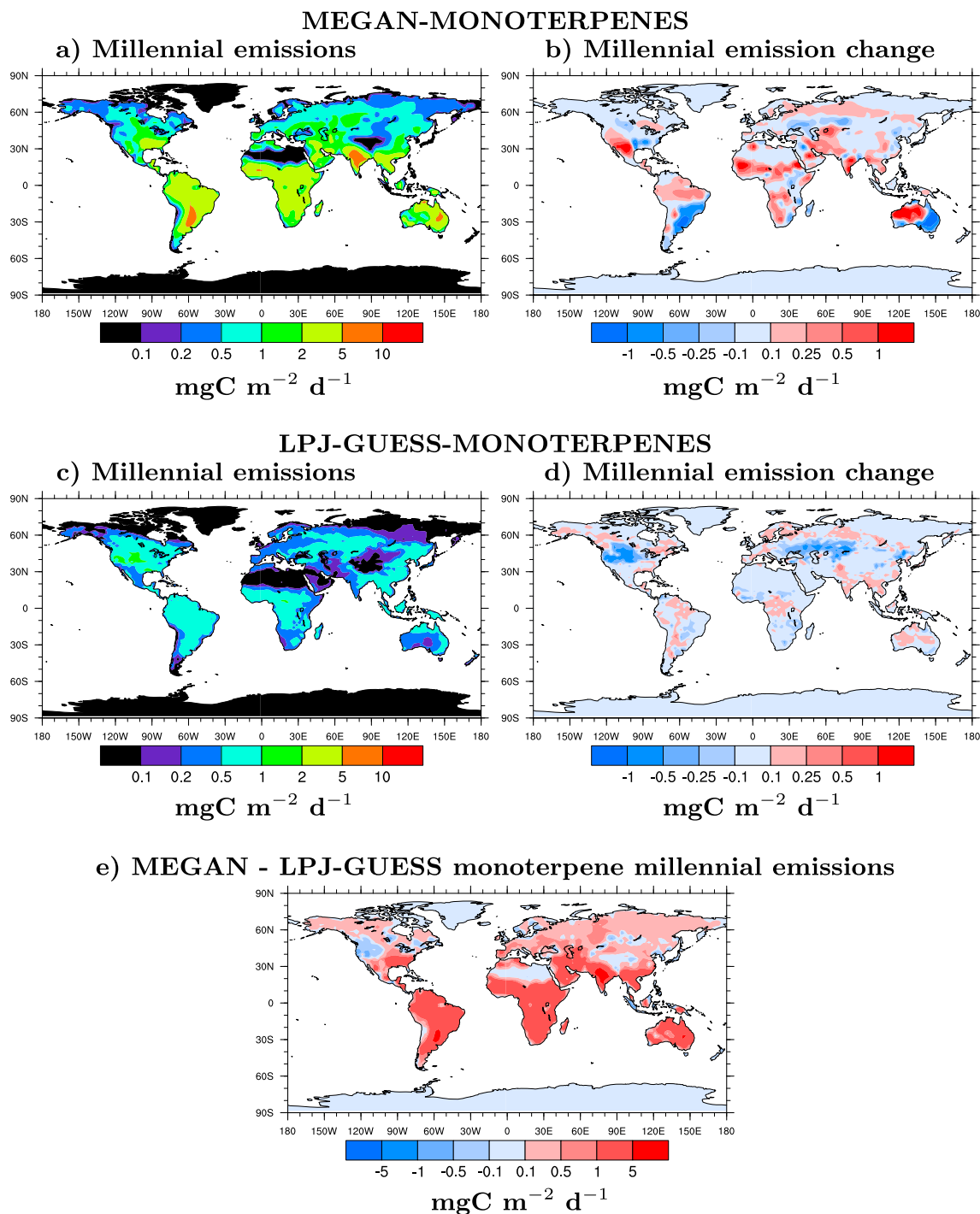
Figure 5. (a) Time-averaged millennial monoterpene emissions in simulation 9 (MF-CO2_OFF). (b) Difference between time-averaged present-day (1980–1990) and time-averaged (1000–1010) monoterpene emissions in simulation 9 (MF-CO2_OFF). (c) Time-averaged millennial monoterpene emissions in simulation 10 (LF-CO2_OFF). (d) Difference between time-averaged present-day (1995–2005) and 950–1050 monoterpene emissions in simulation 10 (LF-CO2_OFF). (e) Absolute difference between the millennial MEGAN monoterpene emissions in simulation 9 (MF-CO2_OFF) and LPJ-GUESS millennial emissions in simulation 10 (LF-CO2_OFF).
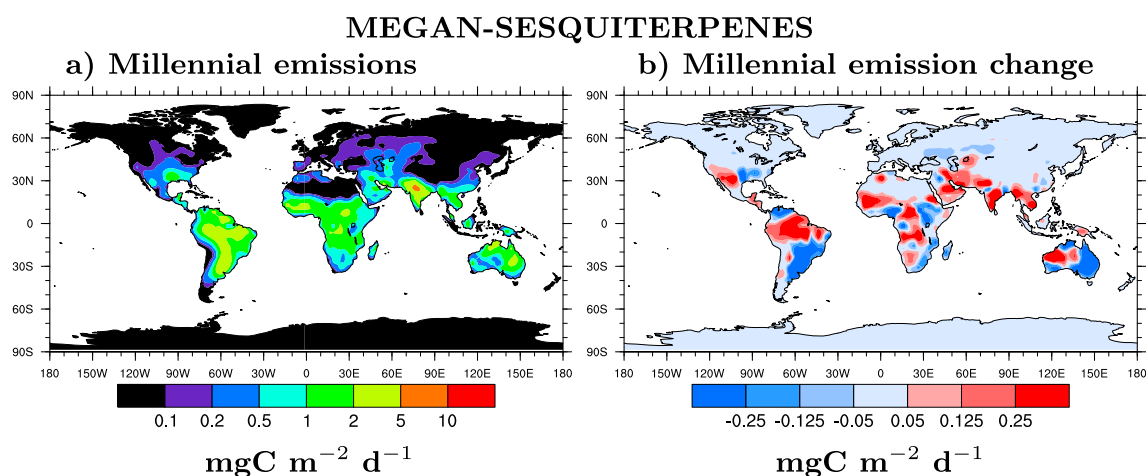
MEGAN-SESQUITERPENES

a) Millennial emissions

b) Millennial emission change

Figure 6. (a) Time-averaged millennial sesquiterpene emissions in simulation 9 (MF-CO2_OFF). (b) Difference between time-averaged present-day (1980–1990) and time-averaged (1000–1010) sesquiterpene emissions in simulation 9 (MF-CO2_OFF).

Although there are clear changes induced by human activities, the changes in the magnitude of emissions are small compared to the uncertainty in absolute emissions associated with the emission factors (see the end of next section for a more detailed discussion on model uncertainty).

3.2. Spatial and Temporal Variability of Terpene Emissions

Figures 4a and 4c show the mean millennial isoprene emissions in simulation 7 (MF-ALL_ON) and simulation 11 (LF-CO2_ON), respectively, corresponding to the best estimates for both models (see Table 5). A major difference between the models is the magnitude of the emissions in most regions. MEGAN emissions are 2 to 3 times larger than LPJ-GUESS emissions in the tropics and in most subtropical regions, probably due to the difference in emissions factors between the models and the use of different climate drivers. Isoprene emissions in both models are dominated by tropical rainforest emissions and decrease with increasing latitude. MEGAN predicts much larger isoprene emissions than LPJ-GUESS in tropical regions and most of the subtropics (red regions in Figure 4e), but LPJ-GUESS emissions over middle and high latitudes are larger than MEGAN. The absolute difference in isoprene emissions between the first and last decades of the millennium in simulations 7 (MF-ALL_ON) and 11 (LF-CO2_ON) are shown in Figures 4b and 4d, respectively. The relative change of isoprene emissions is similar in both models, with a few exceptions in virgin tropical rainforest, where MEGAN predicts an increase in emissions driven by temperature change, but LPJ-GUESS predicts an opposite effect driven by carbon dioxide change.

Figures 5a and 5c show the mean millennial monoterpene emissions in simulation 9 (MF-CO2_OFF) and the simulation 10 (LF-CO2_OFF), respectively (see Table 5). Both models predict a more homogeneous distribution of monoterpene emissions between tropics, subtropics, middle and high latitudes as compared to isoprene emissions. However, MEGAN monoterpene emissions are clearly highest in the tropics and subtropics, in contrast to LPJ-GUESS monoterpene emissions, which are more evenly distributed across all vegetated land. Figure 5e shows that MEGAN emissions are consistently larger than LPJ-GUESS in most locations with exceptions in western North America and central Asia. Figures 5b and 5d show the absolute difference in monoterpene emissions between the end and the beginning of the millennium in simulations 9 (MF-CO2_OFF) and 10 (LF-CO2_OFF), respectively. There is a clear difference in the spatial distribution of the emission change depending on the model used. However, there are some common features between the two emission models: tropical, subtropical, and high-latitude locations show a general positive increment in emissions in both models, which is driven by temperature, while midlatitude emissions show a decreasing trend driven by land cover change.

Figure 6a displays the sesquiterpene millennial emissions in simulation 9 (MF-CO2_OFF). The spatial distribution of the sesquiterpene emissions is somewhere in between that of the isoprene emissions (Figure 4a) and the monoterpene (Figure 5a) emissions. This means that high-latitude vegetation emits a larger sesquiterpene mass fraction than that of isoprene, but less than that of monoterpenes. The reason can be attributed to the difference in the light dependence of the emission of each chemical species. Isoprene

Table 6. Mean Values and Deviations From Preindustrial of Global Mean Surface Air Temperature (SAT), Downward Solar Radiation at Surface (DSRS), Natural Vegetation Cover Fraction, Herbaceous Plant (Crop + Pasture) Cover Fraction, Isoprene (IP), Monoterpene (MT), and Sesquiterpene (ST) Mean Global Emissions During the Medieval Climate Anomaly (MCA), End of the Little Ice Age (LIA)/Preindustrial, and the End of the Twentieth Century[a]

Period	MCA (1000–1200)	End of LIA/ Preindustrial (1750–1850)	End of Twentieth Century (1970–1990)
Global mean SAT (MPI-ESM)	286.7°K	286.4°K	287.2°K
Deviation from preindustrial	+0.3°K	0.0°K	+0.8°K
Global mean DSRS (MPI-ESM)	173.5 W m^{-2}	173.7 W m^{-2}	172.3 W m^{-2}
Deviation from preindustrial	−0.2 W m^{-2}	0.0 W m^{-2}	-1.4 W m^{-2}
Natural vegetation cover fraction	0.63	0.60	0.52
Deviation from preindustrial	+4.3%	0.0%	−14.4%
Herbaceous plant cover fraction	0.13	0.16	0.28
Deviation from preindustrial	−19.0%	0.0%	+73.9%
CO_2 atmospheric concentration	282.6 ppmv	281.3 ppmv	340.3 ppmv
Deviation from preindustrial	+0.5%	0.0%	+21.0%
Global IP emissions (7 (MF-ALL_ON))	779.4 TgC yr^{-1}	725.1 TgC yr^{-1}	633.8 TgC yr^{-1}
Deviation from preindustrial	+7.5%	0.0%	−12.6%
Global IP emissions (11 (LF-CO2_ON))	405.2 TgC yr^{-1}	380.0 TgC yr^{-1}	322.7 TgC yr^{-1}
Deviation from preindustrial	+6.6%	0.0%	−15.1%
Global MT emissions (9 (MF-CO2_OFF))	83.3 TgC yr^{-1}	80.7 TgC yr^{-1}	88.6 TgC yr^{-1}
Deviation from preindustrial	+3.2%	0.0%	+9.8%
Global MT emissions (10 (LF-CO2_OFF))	25.2 TgC yr^{-1}	23.5 TgC yr^{-1}	23.9 TgC yr^{-1}
Deviation from preindustrial	+7.3%	0.0%	+1.6%
Global ST emissions (9 (MF-CO2_OFF))	34.3 TgC yr^{-1}	32.3 TgC yr^{-1}	35.6 TgC yr^{-1}
Deviation from preindustrial	+6.2%	0.0%	+10.2%

[a]The emission mean values are MEGAN and LPJ-GUESS best estimates.

emissions are completely dependent on the availability of light, whereas monoterpenes are almost nondependent of light and sesquiterpene emissions are partially dependent [*Guenther et al.*, 2012].

Table 6 displays the average change in terpene emissions, as well as the change in corresponding input variables to MEGAN and LPJ-GUESS, for three periods of particular interest: namely, the Medieval Climate Anomaly (MCA) from 1000 to 1200, the end of the Little Ice Age (LIA) or preindustrial period from 1750 to 1850, and a recent period from 1970 to 1990. MEGAN isoprene emissions presented in Table 6 are the results from simulation 7 (MF-ALL_ON) and MEGAN monoterpene and sesquiterpene emissions are from simulation 9 (MF-CO2_OFF). Although MEGAN isoprene emissions are about twice as large as LPJ-GUESS isoprene emissions, both models display a similar temporal variability. MEGAN global isoprene emissions during the Medieval Climate Anomaly (MCA) are estimated to be 779 TgC yr^{-1}, which are 7.5% higher than the preindustrial (1750–1850) mean, while LPJ-GUESS emissions are 405.2 TgC yr^{-1}, which is 6.6% higher than the preindustrial (1750–1850) mean. The reasons for higher emissions during the Medieval Climate Anomaly (MCA) are a higher global temperature (+0.3°K) and larger natural vegetation cover fraction (+4.3%) than during preindustrial (1750–1850) times. At the end of the twentieth century (1970–1990), a 14.4% reduction of natural vegetation replaced by crops and pastures and the increase of atmospheric CO_2 as compared to preindustrial (1750–1850) value result in a reduction of isoprene emissions in both models. The global MEGAN and LPJ-GUESS emissions of isoprene during 1970–1990 are 634 TgC yr^{-1} and 323 TgC yr^{-1}, 12.6% and 15.1% less than preindustrial (1750–1850) levels, respectively. These values of isoprene emission reduction fall in the range of previous similar estimates. *Pacifico et al.* [2012] estimated a reduction of 24% and *Tanaka et al.* [2012] estimated a reduction of approximately 3% between 1850s and present day. A possible reason why *Tanaka et al.* [2012] isoprene emission difference is lower than our estimates and the ones estimated by *Pacifico et al.* [2012] could be the use of a different land cover model and not having a CO_2 effect on isoprene emissions.

From our set of simulations it is impossible to tell how large changing downward solar radiation at the surface (DSRS) affected isoprene emissions in the last millennium, but such effects are clearly less than those of changing SAT. To further illustrate this point, we show in Table 6 the millennial variation of SAT and DSRS values used to force MEGAN in simulations 6–9. Global mean DSRS decreases during industrial times and
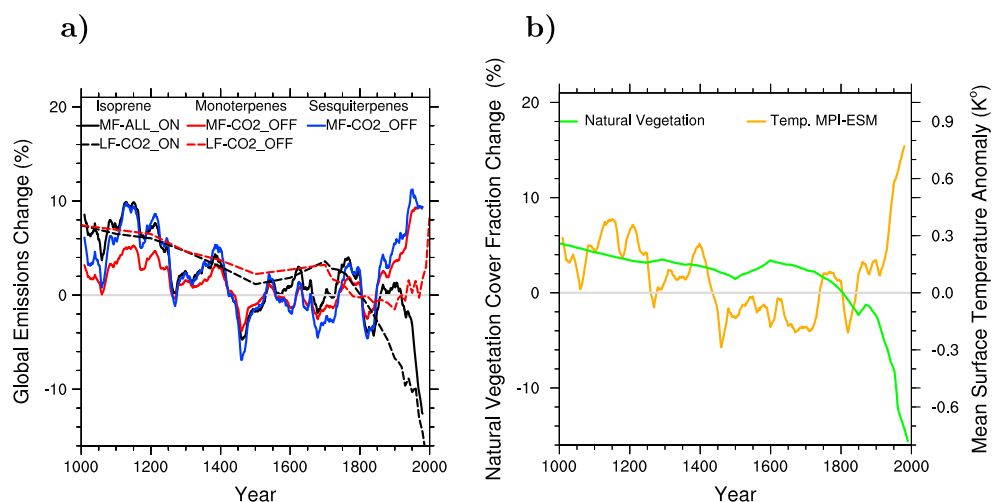
a)   b)

Figure 7. (a) Global emissions deviation from preindustrial mean (1750–1850) of the following: isoprene in simulations 7 (MF-ALL_ON) and 11 (LF-CO2_ON) (solid and dashed black lines), monoterpenes in simulations 9 (MF-CO2_OFF) and 10 (LF-CO2_OFF) (solid and dashed red lines), and sesquiterpenes in simulation 9 (MF-CO2_OFF) (solid blue line). (b) Global natural vegetation cover fraction deviation from preindustrial mean (1750–1850) (solid green line). Mean Surface Air Temperature (SAT) (solid yellow line) deviation from preindustrial mean (1750–1850). All MEGAN and SAT series represent smooth, mean decadal monthly values. Natural vegetation cover series represent yearly mean values. LPJ-GUESS series have 100 year resolution from 1000 to 1700, 20 year resolution from 1700 to 1900, and 10 year resolution from 1900 to 2000.

should have an inhibition effect on isoprene emissions, but on the contrary, isoprene emissions increase following SAT change. A similar effect results in monoterpene and sesquiterpene emissions, suggesting that SAT also dominates in those cases.

The estimates of monoterpene global emissions during the Medieval Climate Anomaly (MCA) are 83 TgC yr^{-1}, 3.2% higher than during preindustrial (1750–1850) times and 25 TgC yr^{-1}, 7.3% higher than preindustrial (1750–1850) levels for MEGAN and LPJ-GUESS, respectively (see Table 6). In contrast to isoprene, larger monoterpene emissions are predicted by both models in more recent days (1970–1990) as compared to preindustrial (1750–1850) values, MEGAN estimates are 89 TgC yr^{-1} (+9.8%), whereas LPJ-GUESS estimates are 24 TgC yr^{-1} (+1.6%). For monoterpene emissions the temperature effect clearly dominates over the land cover effect leading to higher emissions. *Tanaka et al.* [2012] estimated a positive increment from 1854 to 2000 in monoterpene emissions of approximately 3%, a result that agrees with our MEGAN and LPJ-GUESS estimates. Sesquiterpene emissions in MEGAN follow a very similar pattern as the monoterpene emissions. During the Medieval Climate Anomaly (MCA), emissions were 34 TgC yr^{-1}, 6.2% higher than preindustrial (1750–1850) levels, while during the 1970–1990 period the emissions were 36 TgC yr^{-1}, 10.2% higher than preindustrial (1750–1850) levels.

The temporal resolution of MEGAN simulations allowed us to study the difference between the mean emissions in different periods (Table 6). The mean values are significantly different from each other within a 95% confidence interval estimated by a Student's *t* test. The natural short-term variability of emissions cannot explain the change of emissions between different periods. Aside from statistical variability, there are important sources of uncertainty in the emission estimates that cannot be quantified:

1. Uncertainty associated to land cover reconstructions and climatic conditions. This uncertainty is likely largest before 1850.
2. The reduction of ecosystems to general PFT categories with average emission factors. This uncertainty is associated to a large terpene emission variance within a single PFT [*Harley et al.*, 1999; *Klinger et al.*, 1998, 2002].
3. Terpene plant emission and production processes are not fully understood and are manifested in the difference in magnitude and sensitivity to environmental stresses of the terpene emissions estimated by different models. This difference is an evident source of uncertainty in our estimates.
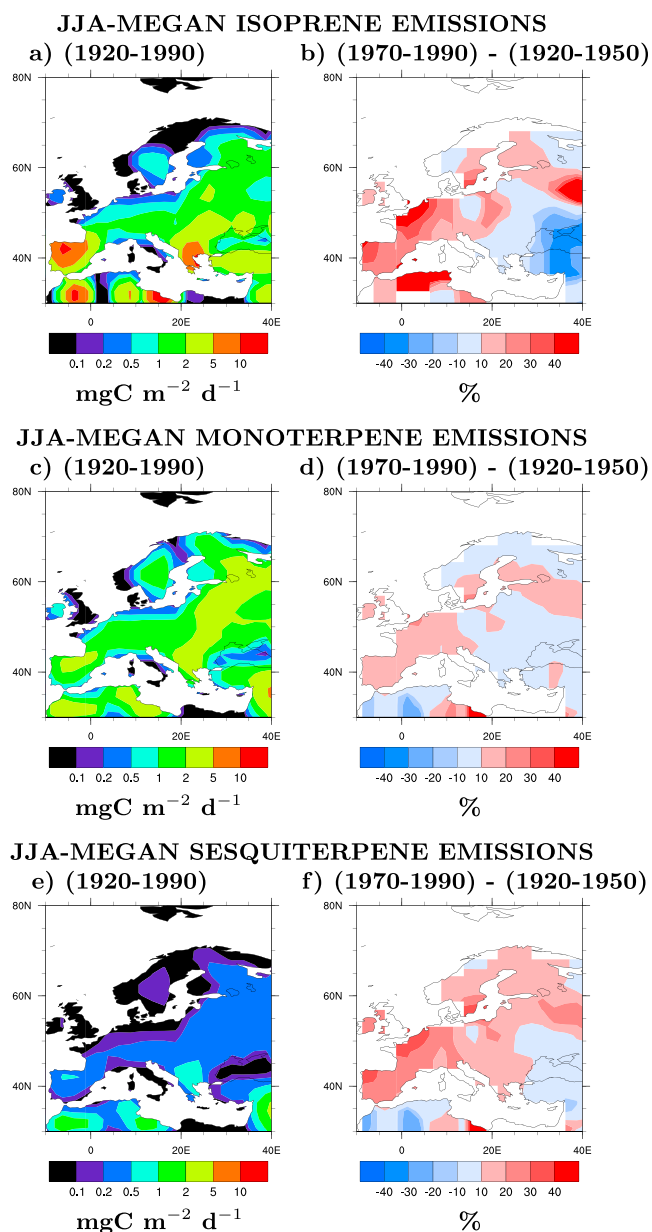
Figure 8. (a) Isoprene emissions in 1920–1990. (b) Change in isoprene emissions between 1970–1990 and 1920–1950. (c) Monoterpene emissions in 1920–1990. (d) Change in monoterpene emissions between 1970–1990 and 1920–1950. (e) Sesquiterpene emissions in 1920–1990. (f) Change in sesquiterpene emissions between 1970–1990 and 1920–1950. Isoprene emissions from simulation 7 (MF-ALL_ON). Monoterpene and sesquiterpene emissions from simulation 9 (MF-CO2_OFF). All values are averages during Northern Hemisphere summer (June, July, and August).

More studies on emission rates for different PFTs and within the same PFT could narrow down the uncertainty and reduce the overall bias in BVOC estimates. A better understanding of the different BVOC emission mechanisms and the controlling factors are essential to improve models in the future. Experimental studies on the variability in the past organic aerosol loading, especially in key areas in the world where major land cover transformations have occurred, could help to consistently evaluate model predictions and build solid constraints to the emission budgets in the past. Currently, almost nonexisting experimental data on BVOC concentrations in the past imposes considerable challenges in evaluating model predictions.

LPJ-GUESS and MEGAN have been individually evaluated against measurements in several studies [*Arneth et al.*, 2007a; *Schurgers et al.*, 2009b; *Guenther et al.*, 2006], and their results have been compared to each other [*Arneth et al.*, 2011; *Guenther et al.*, 2012]. However, independent model evaluation is still largely limited by the lack of observational data. Long-term measurement networks and aircraft observations do not exist for BVOC fluxes, as they do for other gases such as ozone or CO. Furthermore, most of the existing short-term measurements were used to develop the models, and an attempt to evaluate the emissions with those set of measurements would likely be biased.

The large difference between our model estimates is very likely a result of the experimental limitations manifested in the uncertainty of the emission factors for each PFT. Furthermore, this discrepancy could be reduced by scaling the emission factors in both models to show a better agreement on global emissions, and doing so could be easily supported on the uncertainty of the emission factors themselves. However, we see the

difference in our model estimates as an important result that highlights the need for carrying out more numerous and comprehensive experimental work on BVOC emissions. For the reasons mentioned above, we consider that the added value of this study is estimating the response of the emissions over time to changes in the driving variables and the robust regional response observed in certain areas to changes in land cover.

Figure 7a displays the millennial variability of the global MEGAN and LPJ-GUESS best estimates of isoprene and monoterpene emissions, and MEGAN sesquiterpene emissions. To illustrate the main sources of

variability in the global terpene emissions, the change of the driving variables Surface Air Temperature (SAT) and the natural vegetation cover fraction of the KK10 land cover scheme are shown in Figure 7b. By comparing the MEGAN terpene emissions to the mean global SAT, a clear connection is observed for all BVOC species from 1000 to approximately 1800 with small perturbations from land cover change. After 1800, SAT, monoterpene, and sesquiterpene emission series diverge from the isoprene series, suggesting that after 1800, land cover change enhanced by the carbon dioxide effect dominated the isoprene emission variability in MEGAN, whereas SAT is the dominant variable in monoterpene and sesquiterpene emission variability during the whole simulation period. LPJ-GUESS isoprene and monoterpene emission variability follow similar trends as the MEGAN series with a temporal lag after 1800. The lag between the MEGAN and LPJ-GUESS is caused by a lag in the SAT from the CRU data set (used to drive LPJ-GUESS) as compared with the SAT from the climate driver fields used in MEGAN (see Figure S1 in the supporting information) and does not indicate a difference between the models themselves.

3.3. Comparison of Terpene Emission Trends Over Europe and Organic Aerosol Deposition in the Twentieth Century

Alpine ice core data indicate that during European summers a threefold enhancement factor in the concentrations of dissolved organic carbon took place from 1921–1950 to 1971–1988. This enhancement in the organic aerosol fraction was attributed mostly to biogenic sources [*Legrand et al.*, 2013]. Isoprene, monoterpene, and sesquiterpene emissions in simulation 7 (MF-ALL_ON), 9 (MF-CO2_OFF), and 9 (MF-CO2_OFF), respectively, show a general significant increment of European emissions during summer between 1920–1950 and 1970–1990 (Figure 8). In the Alpine region, isoprene, monoterpene, and sesquiterpene emissions grow 10–40%, 10–20%, and 10–30%, respectively. Isoprene emissions are driven by reafforestation and enhanced by surface air temperature (SAT) change, whereas monoterpene and sesquiterpene emission growth is dominated by SAT, with a smaller contribution of reafforestation. It should be borne in mind that the relationship between the dissolved organic material in the ice cores, atmospheric concentrations of BVOCs, and their emissions to the atmosphere are not linear, although most certainly positively correlated with each other. The qualitative comparison presented here is useful in terms of evaluating the trends instead of the magnitude of the emissions. However, a quantitative comparison would require a detailed model study including atmospheric chemistry, aerosol formation, and deposition of the investigated BVOCs. More studies like the one done by *Legrand et al.* [2013] would help modelers in the evaluation and improvement of their emission models.

4. Summary and Conclusions

Humans have modified the land cover well before industrialization and will continue to do so in the future. Industrialization, on the other hand, has lead to substantial increase in the atmospheric carbon dioxide concentrations, resulting in changes in the climate of the Earth. These changes affect BVOC emissions in global and regional scales, thus resulting in a change in the composition of the atmospheric organic mixture. Knowing the amounts and evolution of BVOCs emitted to the atmosphere in the past, present, and future climates is a prerequisite for narrowing down the uncertainty in natural aerosol loadings and furthermore climate sensitivity [*Carslaw et al.*, 2013].

In this work we studied the evolution and driving factors of isoprene and monoterpene emissions during the past millennium, using two independent models: MEGAN and LPJ-GUESS with different descriptions of the emission process and climate drivers. For completeness, we also studied MEGAN predictions for the emissions of sesquiterpenes. According to our best MEGAN estimates for global isoprene emissions decrease from 779 TgC yr^{-1} during years 1000–1200 to 725 TgC yr^{-1} in the industrial period, and furthermore reaching 634 TgC yr^{-1} in the end of the twentieth century, driven mostly by land cover change and enhanced by the carbon dioxide rise in the industrial period. The best estimates for global isoprene emissions using LPJ-GUESS decrease from 405 TgC yr^{-1} to 380 TgC yr^{-1} and finally to 323 TgC yr^{-1} during the same periods, showing an even larger sensitivity to the recent carbon dioxide rise.

The evolution of global monoterpene emissions during the past millennium shows a somewhat different pattern than isoprene: both models predict a slight decrease in emissions between the beginning of the millennium and the preindustrial time (from 83 to 80 TgC yr^{-1} and from 25 to 24 TgC/yr, according to MEGAN and LPJ-GUESS, respectively). MEGAN predicts a substantial increase in monoterpene emissions during the industrial period, reaching 89 TgC yr^{-1} at the end of the twentieth century, while in LPJ-GUESS the

monoterpene emissions stay nearly constant at the level of 24 TgC yr^{-1}. The somewhat different trend predicted by the two models is explained by different sensitivity to temperature versus land cover change: the MEGAN monoterpene predictions are nearly solely determined by the change in global temperature, while in the LPJ-GUESS predictions, the changes in land cover cancel the effects of the rising temperature during the industrial period.

The sesquiterpene emissions predicted by MEGAN follow the global temperature change, showing a decrease from 34 TgC yr^{-1} in 1000–1200 to 32 TgC yr^{-1} in the preindustrial period followed by an increase in the industrial period, and reaching 36 TgC yr^{-1} at the end of the twentieth century. LPJ-GUESS does not simulate sesquiterpene emissions. As shown by the examples above, there is a large difference (about a factor of 2–4) in the absolute magnitude of the emissions predicted by the two models. This difference is explained by the different mechanistic description of the emissions, different vegetation description (offline for MEGAN, online for LPJ-GUESS) in the models, and partly by the different climate drivers used. The differences are significant and highlight the need for observational constraints for improving our understanding of the driving factors behind BVOC emissions [see also, e.g., *Arneth et al.*, 2011]. The models also show clear differences in the spatial distributions of the emissions.

Agriculture and human settlement has lead to transformations in the land cover at different spatial scales throughout the Holocene. Although most of the human-induced change in the BVOC emissions has occurred during the industrial period [*Pacifico et al.*, 2012; *Tanaka et al.*, 2012], this study shows that local, regional, or even continental changes in the emission profiles could have started much earlier. In particular, isoprene emissions have been significantly affected by land cover change throughout the past millennium. Furthermore, our results indicate that the relative magnitudes of isoprene versus monoterpene emissions have changed during the industrial period (see Figure 7). This might have lead to significant differences in the atmospheric oxidation chemistry and biogenic SOA formation between preindustrial and present-day times. Our results therefore suggest that the present-day SOA loadings and properties might not be representative of the preindustrial atmosphere, impacting the predictions of climate sensitivity during the industrial times. This calls for studies coupling these emission estimates to atmospheric transport, chemical processing, state-of-the-art aerosol formation schemes, and the climate.

References

Albrecht, B. A. (1989), Aerosols, cloud microphysics, and fractional cloudiness, *Science*, *245*(4923), 1227–1230, doi:10.1126/science.245.4923.1227.

Andreae, M. O., D. Rosenfeld, P. Artaxo, A. A. Costa, G. P. Frank, K. M. Longo, and M. A. F. Silva-Dias (2004), Smoking rain clouds over the Amazon, *Science*, *303*(5662), 1337–1342, doi:10.1126/science.1092779.

Arneth, A., et al. (2007a), Process-based estimates of terrestrial ecosystem isoprene emissions: Incorporating the effects of a direct CO2-isoprene interaction, *Atmos. Chem. Phys.*, *7*(1), 31–53.

Arneth, A., R. K. Monson, G. Schurgers, U. Niinemets, and P. I. Palmer (2008a), Why are estimates of global terrestrial isoprene emissions so similar (and why is this not so for monoterpenes)?, *Atmos. Chem. Phys.*, *8*(16), 4605–4620, doi:10.5194/acp-8-4605-2008.

Arneth, A., G. Schurgers, T. Hickler, and P. A. Miller (2008b), Effects of species composition, land surface cover, CO2 concentration and climate on isoprene emissions from European forests, *Plant Biol.*, *10*(1), 150–162, doi:10.1055/s-2007-965247.

Arneth, A., G. Schurgers, J. Lathiere, T. Duhl, D. J. Beerling, C. N. Hewitt, M. Martin, and A. Guenther (2011), Global terrestrial isoprene emission models: Sensitivity to variability in climate and vegetation, *Atmos. Chem. Phys.*, *11*(15), 8037–8052, doi:10.5194/acp-11-8037-2011.

Atkinson, R., and J. Arey (2003), Atmospheric degradation of volatile organic compounds, *Chem. Rev.*, *103*(12), 4605–4638.

Carslaw, K. S., O. Boucher, D. V. Spracklen, G. W. Mann, J. G. L. Rae, S. Woodward, and M. Kulmala (2010), A review of natural aerosol interactions and feedbacks within the Earth system, *Atmos. Chem. Phys.*, *10*(4), 1701–1737, doi:10.5194/acp-10-1701-2010.

Carslaw, K., et al. (2013), Large contribution of natural aerosols to uncertainty in indirect forcing, *Nature*, *503*(7474), 67–71.

Ekman, A. M. L., R. Krejci, A. Engström, J. Ström, M. de Reus, J. Williams, and M. O. Andreae (2008), Do organics contribute to small particle formation in the Amazonian upper troposphere?, *Geophys. Res. Lett.*, *35*, L17810, doi:10.1029/2008GL034970.

Engelhart, G. J., A. Asa-Awuku, A. Nenes, and S. N. Pandis (2008), CCN activity and droplet growth kinetics of fresh and aged monoterpene secondary organic aerosol, *Atmos. Chem. Phys.*, *8*(14), 3937–3949, doi:10.5194/acp-8-3937-2008.

Etheridge, D. M., L. P. Steele, R. L. Langenfelds, R. J. Francey, J.-M. Barnola, and V. I. Morgan (1996), Natural and anthropogenic changes in atmospheric CO2 over the last 1000 years from air in Antarctic ice and firn, *J. Geophys. Res.*, *101*(D2), 4115–4128, doi:10.1029/95JD03410.

Fehsenfeld, F., et al. (1992), Emissions of volatile organic compounds from vegetation and the implications for atmospheric chemistry, *Global Biogeochem. Cycles*, *6*(4), 389–430, doi:10.1029/92GB02125.

Guenther, A., S. Archer, J. Greenberg, P. Harley, D. Helmig, L. Klinger, L. Vierling, M. Wildermuth, P. Zimmerman, and S. Zitzer (1999), Biogenic hydrocarbon emissions and landcover/climate change in a subtropical savanna, *Phys. Chem. Earth Part B*, *24*(6), 659–667, doi:10.1016/S1464-1909(99)00062-3.

Guenther, A., T. Karl, P. Harley, C. Wiedinmyer, P. I. Palmer, and C. Geron (2006), Estimates of global terrestrial isoprene emissions using MEGAN (Model of Emissions of Gases and Aerosols from Nature), *Atmos. Chem. Phys.*, *6*(11), 3181–3210, doi:10.5194/acp-6-3181-2006.

Guenther, A. B., X. Jiang, C. L. Heald, T. Sakulyanontvittaya, T. Duhl, L. K. Emmons, and X. Wang (2012), The model of emissions of gases and aerosols from nature version 2.1 (megan2.1): An extended and updated framework for modeling biogenic emissions, *Geosci. Model Dev. Discuss.*, *5*(2), 1503–1560, doi:10.5194/gmdd-5-1503-2012.

Hallquist, M., et al. (2009), The formation, properties and impact of secondary organic aerosol: Current and emerging issues, *Atmos. Chem. Phys.*, *9*(14), 5155–5236, doi:10.5194/acp-9-5155-2009.

Harley, P. C., R. K. Monson, and M. T. Lerdau (1999), Ecological and evolutionary aspects of isoprene emission from plants, *Oecologia*, *118*(2), 109–123, doi:10.1007/s004420050709.

Heald, C. L., M. J. Wilkinson, R. K. Monson, C. A. Alo, G. Wang, and A. Guenther (2009), Response of isoprene emission to ambient co2 changes and implications for global budgets, *Global Change Biol.*, *15*(5), 1127–1140, doi:10.1111/j.1365-2486.2008.01802.x.

Hoyle, C. R., G. Myhre, T. K. Berntsen, and I. S. A. Isaksen (2009), Anthropogenic influence on SOA and the resulting radiative forcing, *Atmos. Chem. Phys.*, *9*(8), 2715–2728, doi:10.5194/acp-9-2715-2009.

Jimenez, J. L., et al. (2009), Evolution of organic aerosols in the atmosphere, *Science*, *326*(5959), 1525–1529, doi:10.1126/science.1180353.

Jungclaus, J. H., et al. (2010), Climate and carbon-cycle variability over the last millennium, *Climate Past Discuss.*, *6*(3), 1009–1044, doi:10.5194/cpd-6-1009-2010.

Kaplan, J. O., G. Folberth, and D. A. Hauglustaine (2006), Role of methane and biogenic volatile organic compound sources in Late Glacial and Holocene fluctuations of atmospheric methane concentrations, *Global Biogeochem. Cycles*, *20*, GB2016, doi:10.1029/2005GB002590.

Kaplan, J. O., K. M. Krumhardt, E. C. Ellis, W. F. Ruddiman, C. Lemmen, and K. K. Goldewijk (2010), Holocene carbon emissions as a result of anthropogenic land cover change, *The Holocene*, doi:10.1177/0959683610386983.

Kaplan, J. O., K. M. Krumhardt, and N. E. Zimmermann (2012), The effects of land use and climate change on the carbon cycle of Europe over the past 500 years, *Global Change Biol.*, *18*(3), 902–914, doi:10.1111/j.1365-2486.2011.02580.x.

Keeling, C. D. (1960), The concentration and isotopic abundances of carbon dioxide in the atmosphere, *Tellus*, *12*(2), 200–203, doi:10.1111/j.2153-3490.1960.tb01300.x.

Keeling, R. F., and S. C. Piper (1996), Global and hemispheric CO2 sinks deduced from changes in atmospheric O2 concentration, *Nature*, *381*, 218–221.

Kerminen, V.-M., et al. (2012), Cloud condensation nuclei production associated with atmospheric nucleation: A synthesis based on existing literature and new results, *Atmos. Chem. Phys.*, *12*(24), 12,037–12,059, doi:10.5194/acp-12-12037-2012.

Kesselmeier, J., and M. Staudt (1999), Biogenic volatile organic compounds (VOC): An overview on emission, physiology and ecology, *J. Atmos. Chem.*, *33*(1), 23–88, doi:10.1023/A:1006127516791.

Klinger, L. F., J. Greenburg, A. Guenther, G. Tyndall, P. Zimmerman, M. M'Bangui, J.-M. Moutsambot, and D. Kenfack (1998), Patterns in volatile organic compound emissions along a savanna-rainforest gradient in Central Africa, *J. Geophys. Res.*, *103*(D1), 1443–1454, doi:10.1029/97JD02928.

Klinger, L. F., Q.-J. Li, A. B. Guenther, J. P. Greenberg, B. Baker, and J.-H. Bai (2002), Assessment of volatile organic compound emissions from ecosystems of China, *J. Geophys. Res.*, *107*(D21), 4603, doi:10.1029/2001JD001076.

Laothawornkitkul, J., J. E. Taylor, N. D. Paul, and C. N. Hewitt (2009), Biogenic volatile organic compounds in the Earth system, *New Phytol.*, *183*(1), 27–51, doi:10.1111/j.1469-8137.2009.02859.x.

Legrand, M., S. Preunkert, B. May, J. Guilhermet, H. Hoffman, and D. Wagenbach (2013), Major 20th century changes of the content and chemical speciation of organic carbon archived in alpine ice cores: Implications for the long-term change of organic aerosol over Europe, *J. Geophys. Res. Atmos.*, *118*, 3879–3890, doi:10.1002/jgrd.50202.

MacFarling Meure, C., D. Etheridge, C. Trudinger, P. Steele, R. Langenfelds, T. van Ommen, A. Smith, and J. Elkins (2006), Law dome CO2, CH4 and N2O ice core records extended to 2000 years BP, *Geophys. Res. Lett.*, *33*, L14810, doi:10.1029/2006GL026152.

Madl, P., and M. Hussain (2011), Lung deposition predictions of airborne particles and the emergence of contemporary diseases-Part II: Lahore Institute of Public Health, *Health*, *2*(3), 101–107.

Makkonen, R., A. Asmi, V.-M. Kerminen, M. Boy, A. Arneth, P. Hari, and M. Kulmala (2012), Air pollution control and decreasing new particle formation lead to strong climate warming, *Atmos. Chem. Phys.*, *12*(3), 1515–1524, doi:10.5194/acp-12-1515-2012.

Mikolajewicz, U., M. Gröger, E. Maier-Reimer, G. Schurgers, M. Vizcaino, and A. M. Winguth (2007), Long-term effects of anthropogenic CO$_2$ emissions simulated with a complex Earth system model, *Clim. Dyn.*, *28*(6), 599–633.

Mitchell, T. D., and P. D. Jones (2005), An improved method of constructing a database of monthly climate observations and associated high-resolution grids, *Int. J. Climatol.*, *25*(6), 693–712.

Monson, R. K., et al. (2007), Isoprene emission from terrestrial ecosystems in response to global change: Minding the gap between models and observations, *Philos. Trans. R. Soc. A*, *365*(1856), 1677–1695.

Niinemets, U., J. D. Tenhunen, P. C. Harley, and R. Steinbrecher (1999), A model of isoprene emission based on energetic requirements for isoprene synthesis and leaf photosynthetic properties for liquidambar and quercus, *Plant Cell Environ.*, *22*(11), 1319–1335, doi:10.1046/j.1365-3040.1999.00505.x.

Niinemets, U., R. K. Monson, A. Arneth, P. Ciccioli, J. Kesselmeier, U. Kuhn, S. M. Noe, J. Peñuelas, and M. Staudt (2010), The leaf-level emission factor of volatile isoprenoids: Caveats, model algorithms, response shapes and scaling, *Biogeosciences*, *7*(6), 1809–1832, doi:10.5194/bg-7-1809-2010.

Olofsson, J., and T. Hickler (2008), Effects of human land-use on the global carbon cycle during the last 6,000 years, *Veg. Hist. Archaeobot.*, *17*(5), 605–615, doi:10.1007/s00334-007-0126-6.

Pacifico, F., G. A. Folberth, C. D. Jones, S. P. Harrison, and W. J. Collins (2012), Sensitivity of biogenic isoprene emissions to past, present, and future environmental conditions and implications for atmospheric chemistry, *J. Geophys. Res.*, *117*, D22302, doi:10.1029/2012JD018276.

Parton, W. J., and J. A. Logan (1981), A model for diurnal variation in soil and air temperature, *Agr. Meteorol.*, *23*, 205–216, doi:10.1016/0002-1571(81)90105-9.

Peñuelas, J., and M. Staudt (2010), BVOCs and global change, *Trends Plant Sci.*, *15*(3), 133–144, doi:10.1016/j.tplants.2009.12.005, Issue: Induced biogenic volatile organic compounds from plants.

Piccot, S. D., J. J. Watson, and J. W. Jones (1992), A global inventory of volatile organic compound emissions from anthropogenic sources, *J. Geophys. Res.*, *97*(D9), 9897–9912, doi:10.1029/92JD00682.

Riipinen, I., et al. (2011), Organic condensation: A vital link connecting aerosol formation to cloud condensation nuclei (CCN) concentrations, *Atmos. Chem. Phys.*, *11*(8), 3865–3878, doi:10.5194/acp-11-3865-2011.

Riipinen, I., T. Yli-Juuti, J. R. Pierce, T. Petäjä, D. R. Worsnop, M. Kulmala, and N. M. Donahue (2012), The contribution of organics to atmospheric nanoparticle growth, *Nat. Geosci.*, *5*(7), 453–458.

Sakulyanontvittaya, T., T. Duhl, C. Wiedinmyer, D. Helmig, S. Matsunaga, M. Potosnak, J. Milford, and A. Guenther (2008), Monoterpene and sesquiterpene emission estimates for the United States, *Environ. Sci. Technol.*, *42*(5), 1623–1629, doi:10.1021/es702274e, pMID: 18441812.

Schurgers, G., et al. (2006), Dynamics of the terrestrial biosphere, climate and atmospheric CO2 concentration during interglacials: a comparison between Eemian and Holocene, *Clim. Past*, *2*(2), 205–220.

Schurgers, G., A. Arneth, R. Holzinger, and A. H. Goldstein (2009a), Process-based modelling of biogenic monoterpene emissions combining production and release from storage, *Atmos. Chem. Phys.*, *9*(10), 3409–3423, doi:10.5194/acp-9-3409-2009.

Schurgers, G., T. Hickler, P. Miller, and A. Arneth (2009b), European emissions of isoprene and monoterpenes from the Last Glacial Maximum to present, *Biogeosci. Discuss.*, *6*(5), 8805–8849.

Schmidt, G. A., et al. (2011), Climate forcing reconstructions for use in PMIP simulations of the last millennium (v1.0), *Geosci. Model Dev.*, *4*(1), 33–45, doi:10.5194/gmd-4-33-2011.

Sitch, S., et al. (2003), Evaluation of ecosystem dynamics, plant geography and terrestrial carbon cycling in the LPJ dynamic global vegetation model, *Global Change Biol.*, *9*(2), 161–185, doi:10.1046/j.1365-2486.2003.00569.x.

Smith, B., I. C. Prentice, and M. T. Sykes (2001), Representation of vegetation dynamics in the modelling of terrestrial ecosystems: Comparing two contrasting approaches within European climate space, *Global Ecol. Biogeogr.*, *10*(6), 621–637, doi:10.1046/j.1466-822X.2001.t01-1-00256.x.

Spracklen, D., et al. (2011), Aerosol mass spectrometer constraint on the global secondary organic aerosol budget, *Atmos. Chem. Phys.*, *11*(23), 12,109–12,136.

Tanaka, K., H.-J. Kim, K. Saito, H. G. Takahashi, M. Watanabe, T. Yokohata, M. Kimoto, K. Takata, and T. Yasunari (2012), How have both cultivation and warming influenced annual global isoprene and monoterpene emissions since the preindustrial era?, *Atmos. Chem. Phys.*, *12*(20), 9703–9718, doi:10.5194/acp-12-9703-2012.

Topping, D., P. Connolly, and G. McFiggans (2013), Cloud droplet number enhanced by co-condensation of organic vapours, *Nat. Geosci.*, *6*(6), 443–446, doi:10.1038/ngeo1809.

Twomey, S. (1977), The influence of pollution on the shortwave albedo of clouds, *J. Atmos. Sci.*, *34*(7), 1149–1152, doi:10.1175/1520-0469(1977).

Valdes, P. J., D. J. Beerling, and C. E. Johnson (2005), The ice age methane budget, *Geophys. Res. Lett.*, *32*, L02704, doi:10.1029/2004GL021004.

Vitousek, P. M., H. A. Mooney, J. Lubchenco, and J. M. Melillo (1997), Human domination of Earth's ecosystems, *Science*, *277*(5325), 494–499, doi:10.1126/science.277.5325.494.

Wu, S., L. J. Mickley, J. O. Kaplan, and D. J. Jacob (2012), Impacts of changes in land use and land cover on atmospheric chemistry and air quality over the 21st century, *Atmos. Chem. Phys.*, *12*(3), 1597–1609, doi:10.5194/acp-12-1597-2012.